

COMPARISON OF HEAT TRANSFER AND PRESSURE DROP BETWEEN ANALYTICAL AND COMPUTATIONAL APPROACHES: A PRELIMINARY STUDY FOR OPTIMAL HEAT EXCHANGER DESIGN

Bağcı Ö.*, Sharif A., Ameer B. and M. De Paepe

*Author for correspondence

Department of Flow, Heat and Combustion Mechanics,
Ghent University,
Sint-Pietersnieuwstraat 41,
9000 Ghent, Belgium
E-mail: ozer.bagci@ugent.be

ABSTRACT

Extended surface areas are indispensable features for compact heat exchanger design. Even one of the simplest, plain-fin-and-tube heat exchangers are still widely studied and used due to their relatively-easy production compared to other types of fin geometries. However, this simplicity only means that there are fewer parameters to consider, compared to those louvered fins for example. Those parameters are the transversal and longitudinal pitches between tubes, fin pitch, fin thickness, inner and outer tube diameters and the number of tube rows, given whether an optimization scheme is required to find a design solution. In this study, the validity of analytical and 3D computational fluid dynamics solutions employing the aforementioned parameters was investigated as a preliminary step to optimal heat exchanger design. The causes of differences between analytical approaches and the associated experimental solutions from previous studies were also sought via simulations. For this purpose, geometric parameters extracted merely from the Reynolds numbers used in those studies, were used to construct a plain-fin-and-tube heat exchanger core. Care was taken so as to employ air velocities remaining in the laminar regime traveling between the fins. It was found that the bounds of the experimental parameters which had been used to define correlations, had a significant impact on the validity of the analytical approach. The three-dimensional model proved to generate viable results with respect to already-published experiments. Since this study constitutes the preliminary step for an optimization scheme, the findings are also accompanied by an extensive literature review on analytical and computational tools.

NOMENCLATURE

A	[m ²]	Area
C	[W/K]	Heat capacity rate
C_p	[J/kgK]	Specific heat at constant pressure
C_r	[-]	Ratio of heat capacity rates, C_{min}/C_{max}
D_c	[m]	Fin collar diameter, $D_o + \delta_f$
D_h	[m]	Hydraulic diameter, $(4A_c L)/A_o$
f	[-]	Friction factor
$F_1...F_3$	[-]	Correlation parameters
G_c	[kg/m ² s]	Mass flux in the contracted area
h	[W/m ² K]	Convective heat transfer coefficient
j	[-]	Colburn factor
k	[W/mK]	Thermal conductivity
L	[m]	Length of the heat exchanger

N	[-]	Number of tube rows
NTU	[-]	Number of transfer units
p	[Pa]	Pressure
$P_1...P_6$	[-]	Correlation parameters
P_f	[m]	Fin pitch
P_l	[m]	Longitudinal tube pitch
P_t	[m]	Transverse tube pitch
q	[W]	Heat transfer
r	[m]	Radius
R	[K/W]	Resistance
T	[K]	Temperature
U	[W/m ² K]	Overall heat transfer coefficient

Special characters

δ_f	[m]	Fin thickness
Δ	[-]	Change
ϵ	[-]	Effectiveness of a heat exchanger
η	[-]	Fin-related efficiency
σ	[-]	Contraction ratio

Subscripts

c	Contracted for area, cold for temperature
f	fin
fr	Frontal
i	Inner
o	Outer
w	Wall
h	Hot
max	Maximum

INTRODUCTION

The real challenge in a heat exchanger analysis is the determination of the transferred heat. If the inlet and outlet temperatures of both hot and cold streams in a heat exchanger are known, the remaining computations are ideally straightforward [1]. If the outlet temperatures are not available, non-dimensional empirical correlations, communicating fluid properties and the exchanger characteristics can be used. Choice of correlation depends on the type of the heat exchanger and whether the streams are mixed inside their own conduits [2]. The heat exchanger effectiveness (ϵ), which is the ratio of the actual heat transfer rate to the maximum possible heat transfer rate, can be referred to as the dependent variable in this correlation. The independent variable in this context, yet still defined by flow, fluid and heat exchanger properties, is the number of transfer units (NTU) which is a measure of "heat transfer size" [2].

The plain-fin-and-tube heat exchangers have also been studied numerically, without the need of providing empirical

inputs such as correlations or coefficients. However, the results of published studies of this sort have also been compared to experimental data directly, or to correlations proven to be in good agreement with those data, as in [3] and [4]. They studied the flow formation along the conduit of a single unit volume of a plain-fin-heat exchanger with design parameters such as fin pitch, tube diameter and number of tube rows. Tutar and Akkoca [3] studied this volume in a time-dependent manner using three-dimensional models. They assumed that the flow was laminar and they based this assumption on previous experimental findings [4, 5]. In [3], the computational runs focused on capturing the evolution of horseshoe vortices around the tubes and eventually their impacts on heat transfer. They also interpreted the pressure loss for different fin pitches and velocities. Their prime cases were heat exchangers with different tube row numbers. It was clearly shown that the horseshoe vortices had a significant influence on heat transfer, results of which were demonstrated locally. However, the unsteady behavior inside the computational domain was induced by introducing a sinusoidal velocity as the inlet boundary condition, and the thermal-hydraulic fluid properties were assumed constant.

A singular representative heat exchanger volume was studied by Borrajo-Peláez et al. [6]. Their purpose was to determine the importance of including the flow and energy transport analysis of liquid stream while the gas stream was already being studied. They compared the results of runs with the liquid stream introduced only as a wall boundary condition to those with liquid-flow zones within tubes. The parameters chosen for demonstrating those two scenarios were the Reynolds number, fin pitch, tube diameter and fin length. It was shown that the choice of including or excluding the liquid stream did not influence the hydrodynamics results of the heat exchanger at all. Nusselt number comparison, on the other hand, showed a divergence as the fin length increased. The representative volume for this study included one full cross section of a tube and two halves of two others which were bounded by the symmetry boundary condition. A boundary condition at the outlet assigning temperature values to the flow returning due to recirculation was introduced by the authors via a user-defined function. In addition, the air properties were assumed constant.

In this study, the analytical model by Wang et al. [7] was coded for plain-fin-and-tube heat exchangers, for staggered tube arrangement, in an iterative manner also employing an ad-hoc empirical effectiveness-number of transfer units relation (ϵ -NTU) for single phase flows [2]. This analytical study was chosen because the main point is to study heat exchangers more compact compared to those published prior to [7] with relatively narrower tubes. The computational model was constructed in a way that its design parameters, such as fin pitch and thickness, tube diameter and number of rows, could be easily changed. The computational domain was also prepared so that, it did not include more than one recurring unit conduit but it was meant to represent the entire heat exchanger volume. Last but not least, the thermal conductivity, viscosity and density were temperature-dependent.

ANALYTICAL APPROACH

Convective heat transfer rate over a surface can be defined as

$$q = hA(T_w - T_c) \quad (1)$$

where h is the convective heat transfer coefficient, A is the exposed area, T_c is the temperature of the relatively-cold stream and T_w is the wall temperature. If the exposed area is increased via placement of fins, the convective heat transfer rate expression becomes

$$q = \eta_o h_o A_o (T_{w,o} - T_c) \quad (2)$$

where η_o , h_o , A_o and $T_{w,o}$ are the overall finned surface efficiency, the convective heat transfer coefficient, the total heat transfer area of the finned surface, and the temperature of the fin base at the surface, respectively. The expressions for the efficiency and the transfer coefficient were adopted from the experimental study conducted by Wang for plain-finned tubes [8].

If the surface being cooled is that of a circular tube, there has to be conductive heat transfer through its wall, as well. One-dimensional steady-state conductive heat transfer for a cylindrical wall is as follows

$$q = k \frac{2\pi L}{\ln(r_w/r_i)} (T_{w,o} - T_{w,i}) \quad (3)$$

where k is the thermal conductivity of the wall material, L is the length of the tube, r_w is the outer radius, r_i is the internal radius and $T_{w,i}$ is the internal wall temperature.

The convective heat transfer over the finless internal surface of the same tube could be easily tailored based on Equation (1) as

$$q = h_i A_i (T_h - T_{w,i}) \quad (4)$$

where h_i is the convective heat transfer coefficient at the relatively-hot-stream side of the heat exchanger, A_i is the area of the internal surface of the tube and T_h is the temperature of the hot stream.

Overall Heat Transfer Coefficient

Equations (2)-(4) represent different paths of the same amount of energy. This fact can be used to obtain a simpler and inclusive form of expression of heat transfer. Let all three equations be modified in a form as follows,

$$\frac{\Delta T}{q} = R \quad (5)$$

Where ΔT is the corresponding temperature difference and R is the corresponding thermal resistance.

When the Equations (2)-(4) are modified accordingly and the sides are gathered for a summation, the equation before any simplification appears

$$\frac{(T_{w,o} - T_c) + (T_{w,o} - T_{w,i}) + (T_h - T_{w,i})}{q} = R_o + R_w + R_i \quad (6)$$

where $R_o = \frac{1}{\eta_o h_o A_o}$, $R_w = \frac{\ln(r_w/r_i)}{2\pi k L}$ and $R_i = \frac{1}{h_i A_i}$.

As a result of further simplification and modification, one obtains an overall heat transfer equation in a similar form of Equation (1)

$$q = UA \Delta T \quad (7)$$

where U is the overall heat transfer coefficient, A is the total heat transfer area, and ΔT is the temperature difference between two temperature values from the end nodes of the heat transfer path, namely T_h and T_c . The value of the overall heat transfer coefficient changes depending on the choice of heat transfer side. However, ΔT has to remain the same. Therefore,

$$UA = U_o A_o = U_i A_i$$

For the design calculations, only the result, UA is needed, and for the related calculations, air-side quantities, namely U_o and A_o were used. Therefore Equation (7) can be expanded into a final form as

$$q = U_o A_o \Delta T \quad (8)$$

where $\Delta T = T_h - T_c$ and

$$U_o = \frac{1}{A_o(R_o + R_w + R_i)} = \frac{1}{A_o \left(\frac{1}{\eta_o h_o A_o} + \frac{\ln(r_w/r_i)}{2\pi k L} + \frac{1}{h_i A_i} \right)}$$

The ε -NTU method

The aforementioned heat transfer can also be interpreted as the heat lost by hot stream or equally, the heat gained by the cold stream, on account of simple energy balance. Therefore the outlet temperatures are bound to be different from the inlet temperatures.

$$q = \dot{m}_h C_{p,h} (T_{h,1} - T_{h,2}) = C_h (T_{h,1} - T_{h,2}) \quad (9)$$

$$q = \dot{m}_c C_{p,c} (T_{c,2} - T_{c,1}) = C_c (T_{c,2} - T_{c,1}) \quad (10)$$

where \dot{m} is the mass flow rate, C_p is the specific heat and C is the heat capacity rate. The subscripts 1 and 2 denote the inlet and outlet, respectively. As can be guessed by interpreting the two equations above, the stream with the lower heat capacity rate experiences the larger temperature change. In addition to this deduction, an approach was used to determine the highest possible heat transfer (q_{max}) for a heat exchanger. This approach suggested that the outlet temperatures of the streams were equal to each other if the flow conduits were infinitely long [9]. Then, the temperature difference needs to be chosen as that between the inlet temperatures, and the heat capacity rate as that with the lower value since this thermal process is undergone by the same stream.

$$q_{max} = C_{min} (T_{h,1} - T_{c,1}) \quad (11)$$

where q_{max} is the highest, thermodynamically attainable heat transfer and C_{min} is the lower heat capacity rate among C_h and C_c .

The effectiveness of a heat exchanger can now be defined as follows,

$$\varepsilon = \frac{q}{q_{max}} \quad (12)$$

This non-dimensional number is a function of number of transfer units (NTU) and the ratio of the lower heat capacity rate to the higher heat capacity rate (C_r). Since the plain-fin-heat exchangers are chosen as the object of study, and both hot and cold streams are unmixed in the conduits, the effectiveness is defined as follows,

$$\varepsilon = 1 - \exp\left(\frac{NTU^{0.22}(\exp(-C_r NTU^{0.78}) - 1)}{C_r}\right) \quad (13)$$

where $NTU = \frac{U_o A_o}{C_{min}}$, and $C_r = \frac{C_{min}}{C_{max}}$.

The heat exchanger geometry

The plain-fin-and-tube heat exchanger has a structure allowing a cross-flow of two different fluids. Air is allowed to flow through the conduit with the surface area increased via closely-placed fins in a linear array.

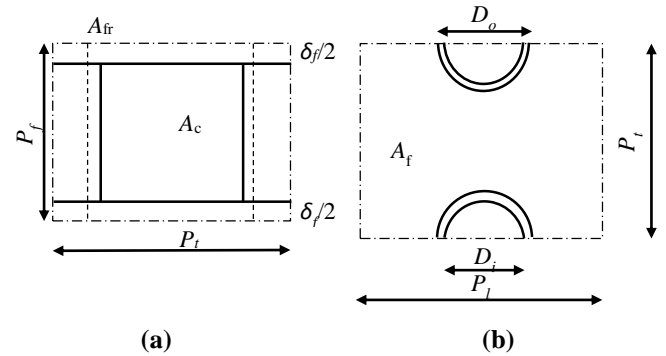


Figure 1 Representative views of a plain-fin-and-tube heat exchanger: (a) Front view of a unit volume showing the contracted area (A_c) and the complete frontal area (A_{fr}), (b) Top view of the same unit volume showing the fin area.

Figure 1 (a) indicates the plane perpendicular to the air-flow direction. Therefore P_t denotes the transverse tube pitch, which is the distance between two tubes aligned in the transverse direction with respect to air flow. P_f is the fin pitch, which is the distance between each fin and δ_f is the fin thickness. Figure 1 (b), on the other hand, shows P_l , the longitudinal tube pitch, which is the distance between the tube rows. The inner and outer diameters of the tubes, D_i and D_o , respectively, are also visible.

Calculation of the surface areas

The contraction ratio is required to determine the interstitial or core velocity between the tubes. It is in fact simply the contracted area A_c divided by the frontal area, A_{fr} :

$$\sigma = \frac{A_c}{A_{fr}} \quad (14)$$

where $A_{fr} = P_t P_f$ and $A_c = (P_f - \delta_f)(P_t - D_c)$. D_c is the fin collar diameter, which is the expanded outer diameter of the tube, according to Wang's correlations [8].

Fin surface area, required to find the fin efficiency, was calculated taking into account the entire line of unit volumes along the air flow, disregarding the number of transverse tube passes.

$$A_f = 2 \left(P_t N P_l - \frac{N \pi D_c^2}{4} \right) + 2 P_t \delta_f \quad (15)$$

The air-side total heat transfer area was found as follows,

$$A_o = N(P_f - \delta_f) \pi D_c + 2 \left(P_t N P_l - \frac{N \pi D_c^2}{4} \right) + 2 P_t \delta_f \quad (16)$$

Wang's correlations

Wang derived expressions for some of the key variables found in the equations above, which are the overall fin efficiency (η_o), air-side convective heat transfer coefficient (h_o), and also pressure loss (ΔP) [7, 8]. The definition of the water-side convective heat transfer coefficient (h_i) was proposed by Gnielinski [10].

The overall fin efficiency is calculated as follows,

$$\eta_o = 1 - \frac{A_f}{A_o} (1 - \eta_f) \quad (17)$$

Where A_f is the area of the fin surface and η_f is the efficiency of a single fin

$$\eta_f = \frac{\tanh(mr\phi)}{mr\phi} \quad (18)$$

where $m = \sqrt{\frac{2h_o}{k_f \delta_f}}$ and $\phi = \left(\frac{Re_{eq}}{r} - 1 \right) [1 + 0.35 \ln(Re_{eq}/r)]$

$\frac{Re_{eq}}{r} = 1.27 \frac{X_M}{r} \left(\frac{X_L}{X_M} - 0.3 \right)^{1/2}$ and $X_M = \frac{P_t}{2}$, $X_L = \frac{\sqrt{(P_t/2)^2 + P_l^2}}{2}$

where P_t and P_l are the transverse and longitudinal tube pitches, respectively.

The air-side convective heat transfer coefficient, h_o , is calculated approximating the Colburn factor,

$$h_o = \frac{\rho V_{max} C_{p,air} j}{Pr^{2/3}} \quad (19)$$

Where ρ is the density of air, V_{max} is the interstitial velocity, which is the heightened value of the inlet velocity due to contraction of the flow field, Pr is the Prandtl number, j is the Colburn factor which can be found via the correlation by Wang [7] depending on the number of tube rows. Both of the correlations for Colburn factor and friction factor were found by Wang [7] who used 8 different studies in a data bank. Those studies included results with different tube row numbers which were 1, 2, 3, 4, 5, and 6, with the corresponding number of studies which were 19, 18, 3, 26, 1 and 6, respectively, [8, 11-16].

If $N=1$, then

$$j = 0.11 Re_{D_c}^{-0.29} \left(\frac{P_t}{P_l} \right)^{P_1} \left(\frac{P_f}{D_c} \right)^{-1.084} \left(\frac{P_f}{D_h} \right)^{-0.786} \left(\frac{P_f}{P_t} \right)^{P_2} \quad (20)$$

where Re_{D_c} is the Reynolds number based on fin collar diameter $D_c = D_o + \delta_f$, N is the number of tube rows and D_h is the hydraulic diameter $\left(\frac{4A_{cL}}{A_o} \right)$. P_1 and P_2 are calculated as follows,

$$P_1 = 1.9 - 0.23 \ln(Re_{D_c}) \text{ and} \\ P_2 = -0.236 - 0.126 \ln(Re_{D_c}).$$

If $N \geq 2$, then

$$j = 0.086 Re_{D_c}^{P_3} N^{P_4} \left(\frac{P_f}{D_c} \right)^{P_5} \left(\frac{P_f}{D_h} \right)^{P_6} \left(\frac{P_f}{P_t} \right)^{-0.93} \quad (21)$$

where

$$P_3 = -0.361 - \frac{0.042N}{\ln(Re_{D_c})} + 0.158 \ln \left(N \left(\frac{P_f}{D_c} \right)^{0.41} \right),$$

$$P_4 = -1.224 - \frac{0.076 \left(\frac{P_l}{D_h} \right)^{1.42}}{\ln(Re_{D_c})},$$

$$P_5 = -0.083 + \frac{0.058N}{\ln(Re_{D_c})} \text{ and}$$

$$P_6 = -5.735 - 1.21 \ln \left(\frac{Re_{D_c}}{N} \right).$$

Pressure loss correlation was presented as follows [7],

$$\Delta P = \left(\frac{G_c^2}{2\rho_1} \right) \left[\left(f \frac{A_o \rho_1}{A_c \rho_m} \right) + (1 + \sigma^2) \left(\frac{\rho_1}{\rho_2} - 1 \right) \right] \quad (22)$$

where σ is the contraction ratio of the flow field, G_c is the mass flux in the contracted area (ρV_{max}). ρ_1 , ρ_2 and ρ_m are the air-inlet and outlet density, and the average density based on the former two. f is the friction factor correlated as follows [7],

$$f = 0.0267 Re_{D_c}^{F_1} \left(\frac{P_t}{P_l} \right)^{F_2} \left(\frac{F_p}{D_c} \right)^{F_3} \quad (23)$$

where

$$F_1 = -0.764 + 0.739 \frac{P_t}{P_l} + 0.177 \frac{P_f}{D_c} - \frac{0.00758}{N},$$

$$F_2 = -15.689 + \frac{64.021}{\ln(Re_{D_c})} \text{ and}$$

$$F_3 = 1.696 - \frac{15.695}{\ln(Re_{D_c})}.$$

THE COMPUTATIONAL APPROACH

Since the analytical model by Wang et al. was based on plain-fin-and-tube heat exchangers with staggered distribution of tubes [7, 8], the geometric features for a unit volume for both analytical and computational parts were decided upon accordingly. Because the tubes were distributed in a staggered fashion, the unit heat exchanger volume had two halves of two tubes located at non-zero longitudinal and transverse distances with respect to flow direction. Each one of these tubes had a cross section bounded by surfaces to which symmetric boundary condition was assigned, as seen in Figure 2.

The entire computational domain consisted of both fluid and solid zones. The lateral surfaces of this domain were considered symmetric, on the other hand, top and the bottom surfaces were periodic. The use of such an elementary volume was studied in conjunction with its proximity to the edges of a heat exchanger by DeJong and Jacobi [17] and they found this volume behaved differently only for several fins away from the wall. This effect was also pronounced in the study of Wang et al. [18].

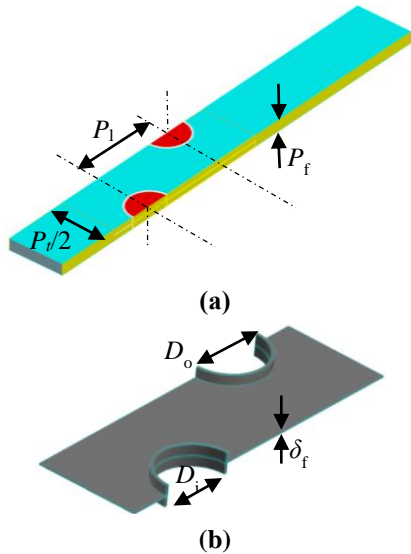


Figure 2 The geometry of the computational domain: (a) The entire domain including solid and fluid zones, (b) Solid zone including the fin and the tubes.

The inlet and outlet boundary conditions for the air stream were chosen to be velocity inlet and pressure outlet, respectively. This was also the case for the water conduits, namely tubes. The constant air inlet velocities changed between 1 and 5 m/s. This value was always 2.87 m/s for the tubes, for providing the same flow rate as that in the study by Wang et al. [7]. The number of the tubes changed between 2 and 6.

The flow between the fins was considered laminar, as inspired by previous studies [3, 6, 19, 20]. However, the fluid zones located in the upstream and the downstream of the fin were considered turbulent because of the mixing at the outlet of the complete heat exchanger surface and the free shear layers. Therefore a $k-\epsilon$ turbulence model and an enhanced wall function were employed. Thanks to this assumption, the viscosity had a higher value to prevent any recirculation after a tube and reaching the outlet, thus, causing numerical oscillations.

The computational grid of the domain was able to be generated in a parametric manner with help of a code producing an input file for the mesh software Gambit. The grids for geometries with two tube rows included 564102 volume mesh elements, the grids with 6 rows, on the other hand, included 1328226 cells.

RESULTS

Figure 3 shows the surface heat transfer coefficient distribution along the fin surface. This coefficient is merely qualitative as it is found using a constant reference value instead of bulk temperature. The highest-heat-transfer zones exist at the upstream side of the fin surface because of the developing boundary layer and the upstream sides of the tubes because of horseshoe vortices which were then replaced by recirculation vortices after the tubes which inhibit the heat transfer, as also observed in [6].

The results of the analytical model and the computational model were compared with each other for velocities 1-5 m/s through 2 rows of tubes and 1-3 m/s through 6 rows of tubes. The

velocities were not any higher for the larger number of rows due to computational oscillations.

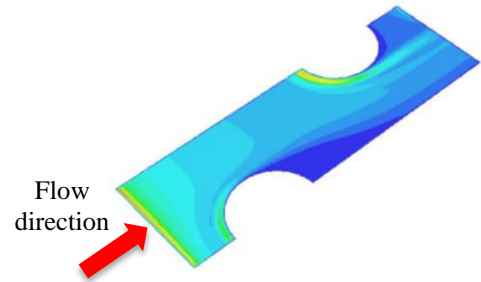


Figure 3 Surface heat transfer coefficient distribution

The analytical model was tested by comparing it to the computational model. Figure 4 (a) shows a very good agreement between the pressure loss results of the analytical and computational models. However, as seen in Figure 4 (b), heat transfer trend is different at relatively high velocities. This phenomenon can be attributed to the same inlet temperature for both tubes in the computational domain. In reality, one of those streams enters the corresponding volume with a diminished temperature due to former heat loss.

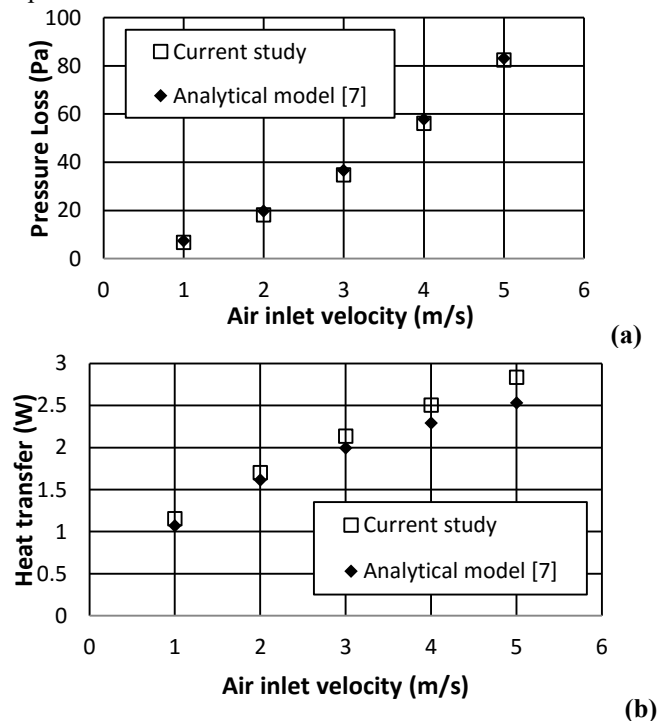


Figure 4 Results for flow through 2 rows of tubes: (a) Pressure loss, (b) Heat transfer

Unlike the results for 2 tube rows exhibiting resemblance, 6-tube-row cells depict significant disagreements for both pressure loss and heat transfer. This failure of applicability can be related to the attempt to use the analytical model at the higher end of the correlation range with respect to tube rows because there were only 6 results published for 6-tube-row heat exchangers, out of 74 results used to construct the correlation. In

Figure 5 (a) and (b), the curve fits can also be seen, exhibiting a high fidelity for the attributed points.

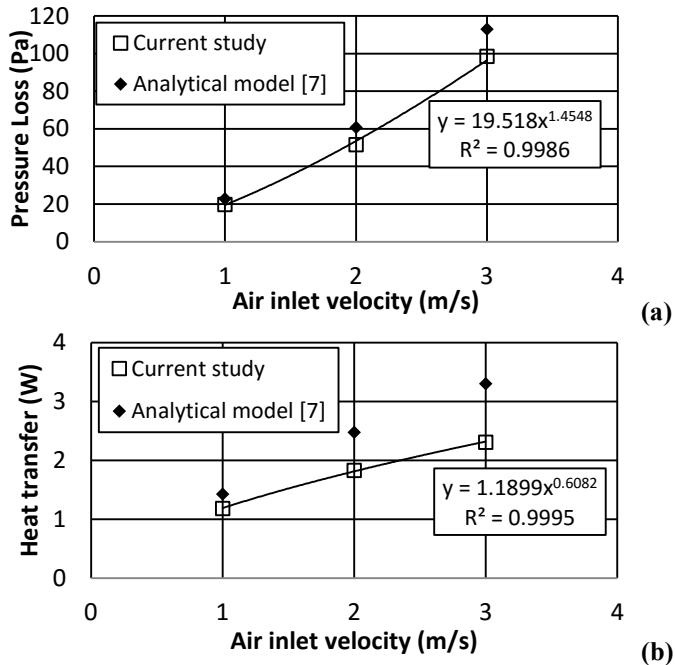


Figure 5 Results for flow through 6 rows of tubes: (a) Pressure loss, (b) Heat transfer

CONCLUSION

An analytical model for a set of plain-fin-heat exchangers was built on correlations based on experiments. Geometric and computational fluid dynamics models were also generated to repeat the results of the analytical data so that a trustworthy tool for later use for optimization schemes would be obtained. The models exhibited good agreement within the lower end of the tube-row range. However this agreement failed when the number of the tubes were increased to the highest number for the data bank. The computational model can be further developed by including more realistic water inlet temperatures by taking into account the size of the heat exchanger.

ACKNOWLEDGMENTS

This work was supported by the Agency for Innovation by Science and Technology (IWT) under project EUFORIA, for which the authors are very thankful.

REFERENCES

- [1] Kakac S., Liu H. and Pramuanjaroenkij A. *Heat exchangers: selection, rating, and thermal design*: CRC press, 2012
- [2] Kays W.M. and London A.L., *Compact heat exchangers* Vol., No. 1984, pp
- [3] Tutar M. and Akkoca A., Numerical analysis of fluid flow and heat transfer characteristics in three-dimensional plate fin-and-tube heat exchangers *Numerical Heat Transfer, Part A: Applications* Vol. 46, No. 3, 2004, pp 301-321
- [4] Romero-Méndez R., Sen M., Yang K. and McClain R., Effect of fin spacing on convection in a plate fin and tube heat exchanger *International Journal of Heat and Mass Transfer* Vol. 43, No. 1, 2000, pp 39-51
- [5] Jang J.-Y., Wu M.-C. and Chang W.-J., Numerical and experimental studies of threedimensional plate-fin and tube heat exchangers *International Journal of Heat and Mass Transfer* Vol. 39, No. 14, 1996, pp 3057-3066
- [6] Borrajo-Peláez R., Ortega-Casanova J. and Cejudo-López J., A three-dimensional numerical study and comparison between the air side model and the air/water side model of a plain fin-and-tube heat exchanger *Applied Thermal Engineering* Vol. 30, No. 13, 2010, pp 1608-1615
- [7] Wang C.-C., Chi K.-Y. and Chang C.-J., Heat transfer and friction characteristics of plain fin-and-tube heat exchangers, part II: Correlation *International Journal of Heat and Mass Transfer* Vol. 43, No. 15, 2000, pp 2693-2700
- [8] Wang C.-C. and Chi K.-Y., Heat transfer and friction characteristics of plain fin-and-tube heat exchangers, part I: new experimental data *International Journal of Heat and Mass Transfer* Vol. 43, No. 15, 2000, pp 2681-2691
- [9] Bergman T.L., Incropera F.P. and Lavine A.S. *Fundamentals of heat and mass transfer*: John Wiley & Sons, 2011
- [10] Gnielinski V., New equations for heat and mass-transfer in turbulent pipe and channel flow *International chemical engineering* Vol. 16, No. 2, 1976, pp 359-368
- [11] Wang C.-C., Lee C.-J., Chang C.-T. and Chang Y.-J., Some aspects of plate fin-and-tube heat exchangers: with and without louvers *Journal of Enhanced Heat Transfer* Vol. 6, No. 5, 1999, pp
- [12] Wang C.-C., Chang J.-Y. and Chiou N.-F., Effects of waffle height on the air-side performance of wavy fin-and-tube heat exchangers *Heat Transfer Engineering* Vol. 20, No. 3, 1999, pp 45-56
- [13] Wang C.-C., Chang Y.-J., Hsieh Y.-C. and Lin Y.-T., Sensible heat and friction characteristics of plate fin-and-tube heat exchangers having plane fins *International Journal of Refrigeration* Vol. 19, No. 4, 1996, pp 223-230
- [14] Rich D.G., The effect of fin spacing on the heat transfer and friction performance of multi-row, plate fin-and-tube heat exchangers *ASHRAE Trans* Vol. 79, No. 2, 1973, pp 137-145
- [15] Rich D.G. *The effect of the number of tube rows on heat transfer performance of smooth plate fin-and-tube heat exchangers* 1975
- [16] Seshimo Y. and Fujii M. An experimental study of the performance of plate fin and tube heat exchangers at low Reynolds number. In: *Proceeding of the 3rd ASME/JSME Thermal Engineering Joint Conference*, 1991, p^pp 449-454
- [17] DeJong N. and Jacobi A., Flow, heat transfer, and pressure drop in the near-wall region of louvered-fin arrays *Experimental Thermal and Fluid Science* Vol. 27, No. 3, 2003, pp 237-250
- [18] Wang Y.Q., Dong Q.-W., Liu M.-S. and Wang D., Numerical Study on Plate-Fin Heat Exchangers with Plain Fins and Serrated Fins at Low Reynolds Number *Chemical engineering & technology* Vol. 32, No. 8, 2009, pp 1219-1226
- [19] He Y.-L., Tao W., Song F. and Zhang W., Three-dimensional numerical study of heat transfer characteristics of plain plate fin-and-tube heat exchangers from view point of field synergy principle *International Journal of Heat and Fluid Flow* Vol. 26, No. 3, 2005, pp 459-473
- [20] Xu W. and Min J., Numerical predictions of fluid flow and heat transfer in corrugated channels using time-dependent and time-independent flow models *Journal of Enhanced Heat Transfer* Vol. 11, No. 4, 2004, pp